

Electrical transport and high pressure studies on bulk $\text{Ge}_{20}\text{Te}_{80}$ glass

G PARTHASARATHY, A K BANDYOPADHYAY,* S ASOKAN and
E S R GOPAL

Department of Physics, Indian Institute of Science, Bangalore 560012, India

* Present address: National Physical Laboratory, Hillside Road, New Delhi 110012, India

MS received 6 August 1983; revised 4 April 1984

Abstract. The electrical resistivity of bulk $\text{Ge}_{20}\text{Te}_{80}$ has been measured as a function of pressure and temperature. At 5 GPa, an amorphous semiconductor-to-crystalline metal transition has been observed. The sample recovered from the high pressure cell, after the application of 7 GPa, has a face-centred cubic structure with a lattice constant of 6.42 Å. In crystalline sample, the semiconductor-to-metal transition occurs at 7 GPa. The thermoelectric power has also been measured for glassy samples in the temperature range 300–240 K.

Keywords. High pressure effects on solids; chalcogenide glass; semiconductor-to-metal transition; pressure-induced crystallization.

PACS No. 72.80

1. Introduction

There has been some amount of work on the effect of pressure on the transport mechanism of amorphous semiconductors. A number of amorphous materials have been studied which includes amorphous germanium and silicon (Shimomura *et al* 1974), amorphous arsenic (Elliot *et al* 1977) and amorphous As_2Te_3 (Sakai and Fritzsche 1977). Most of these materials were studied in thin film form, where the electrical properties depend upon the condition of preparation like rate of evaporation, substrate temperature etc. Very few experimental data have been reported on the effect of pressure on bulk chalcogenide glasses (Johnson and Quinn 1978; Geetha Ramani *et al* 1979; Nakamura *et al* 1975; Bhatia *et al* 1983). The usual and interesting behaviour of these glasses is that the material undergoes a semiconductor-to-metal transition under high pressure (Minomura 1982; Prasad *et al* 1984; Parthasarathy and Gopal 1984). The crystalline phase of some of the materials also undergoes the semiconductor-to-metal transition, but the transition pressure seems to be always higher than that for the amorphous phase (Minomura 1982).

In the present paper, we report a pressure-induced semiconductor-to-metal transition in bulk $\text{Ge}_{20}\text{Te}_{80}$ glass and crystalline $\text{Ge}_{20}\text{Te}_{80}$ sample. Earlier work on the pressure dependence on the electrical resistivity was only up to 0.3 GPa (Nakamura *et al* 1975). As far as we know, this is the first high pressure study on this system. The observed transitions have been detected by the drastic change in the electrical resistivity and the structural analysis of the pressure quenched samples. We also report the temperature dependence of the thermoelectric power of bulk GeTe_4 glass.

2. Experimental

2.1 Sample preparation and characterization

Cornet (1976) reported that the bulk glass forming region of the $\text{Ge}_x\text{Te}_{1-x}$ system ranges from $x = 0.13$ to $x = 0.22$. The present sample $\text{Ge}_{20}\text{Te}_{80}$ was prepared by direct reaction of the individual elements Ge (99.999%) and Te (99.999%). The stoichiometric compositions of the individual elements were first mixed and then filled inside a quartz tube (thickness 0.5 mm) which has a rectangular cross-section to increase the cooling rate. The ampoule was evacuated (10^{-6} torr) and purged with argon gas several times to reduce the presence of residual oxygen and finally sealed in an argon environment. The sample was heated up to 1300 K for about 36 hr. A special arrangement was made to continuously rotate the ampoule at a speed of 10 rpm. The ampoule was then quenched in an ice-water mixture.

The glassy nature of the prepared samples was confirmed by x-ray and electron diffraction studies. Differential scanning calorimetry (Perkin-Elmer DSC-2) analysis

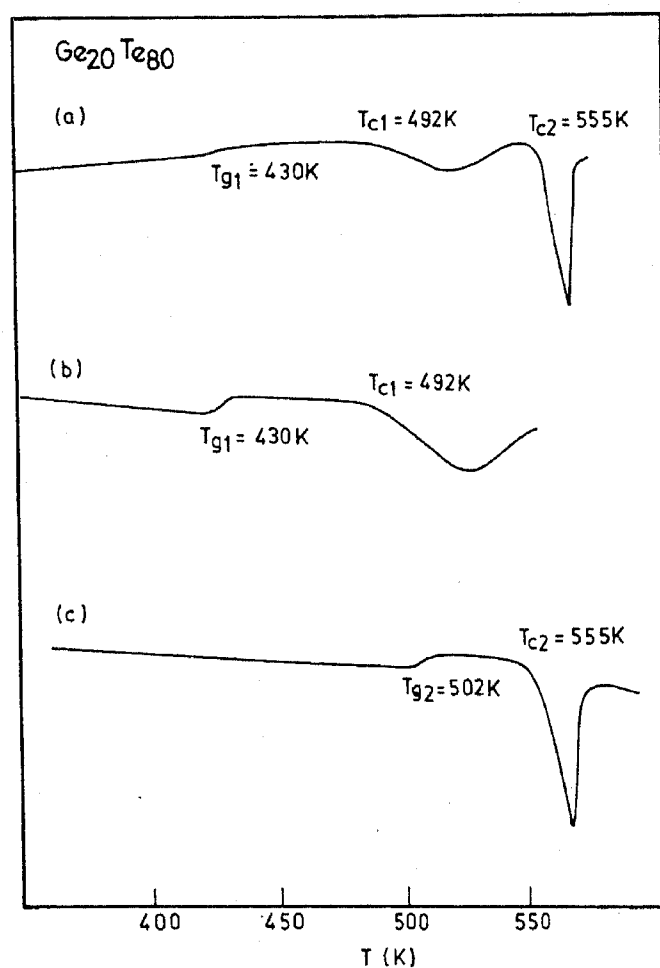


Figure 1. DSC traces taken for $\text{Ge}_{20}\text{Te}_{80}$ glass. Heating rate 20 K/min (dH/dT) = 10 mcal/sec. (a) Continuous heating until complete crystallization, (b) Continuous heating up to first crystallization, (c) Samples of (b) cooled down to room temperature and re-heating until complete crystallization. T_g 's are glass transition temperatures and T_c 's are crystallization temperatures.

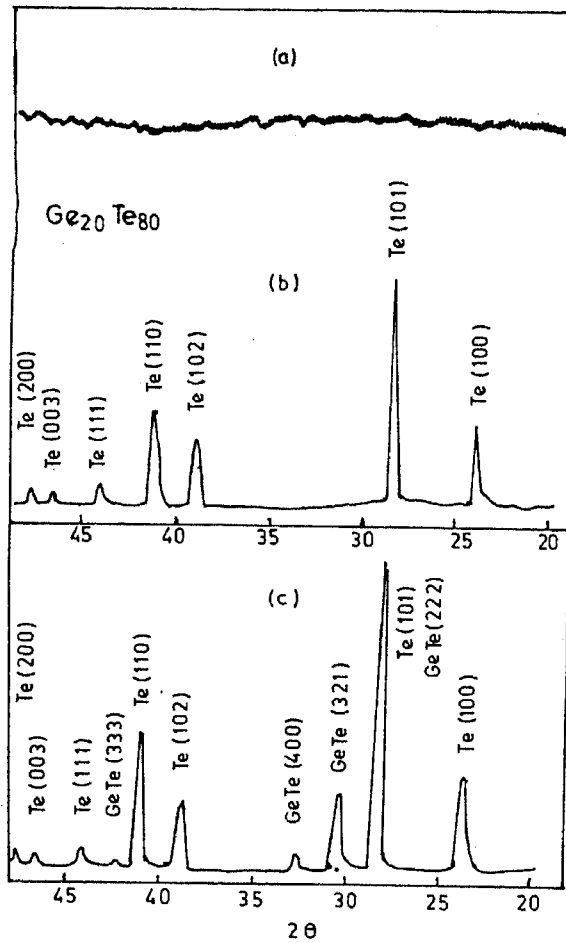


Figure 2. X-ray diffractogram of (a) amorphous $\text{Ge}_{20}\text{Te}_{80}$, (b) after the first crystallization and (c) after complete crystallization of $\text{Ge}_{20}\text{Te}_{80}$ sample.

was also carried out over the temperature range 300–600 K at a rate of 20 K/min. The sample exhibits a double stage crystallization phenomenon. The DSC traces are shown in figure 1 and the x-ray diffraction pattern at different stages of crystallization is shown in figure 2. The details about the double-stage crystallization phenomena observed in this sample have been discussed elsewhere (Parthasarathy *et al* 1984a).

2.2 High pressure experiments

The electrical resistivity was measured under high pressure (up to 8 GPa) with a Bridgman anvil set-up described elsewhere (Bandyopadhyay *et al* 1980; Parthasarathy *et al* 1984b). Pressure was calibrated at room temperature as well as at low temperatures by studying the polymorphic phase transitions of bismuth, ytterbium and thallium (Parthasarathy *et al* 1984b). The specimen was embedded in a steatite pressure transmitting medium and surrounded by a heat-treated pyrophyllite gasket. For recovering the pressure quenched sample sodium chloride was used as a pressure transmitting medium. The sample was recovered by dissolving sodium chloride medium in double-distilled water.

2.3 Electrical measurements

The resistance was measured by a four-probe method. The resistivity at room temperature and atmospheric pressure was measured by the van der Pauw technique. A Keithley electrometer (model No. 616), a Keithley constant current source (model No. 225) and a Keithley digital multimeter (model No. 177) were used as measuring instruments. The thermoelectric power was measured in a conventional set-up. The sample was placed between two copper rods. Two small heater wires, electrically insulated but thermally well connected with the sample, were wound around. A differential thermocouple was used to measure the temperature gradient across the sample. The whole system was placed on a copper block and the temperature was usually controlled within ± 0.1 K. The thermo EMF was measured using a Keithley microvoltmeter. Copper-constantan thermocouples were used to measure the temperature. The temperature region of investigations was limited because of the high resistance of the sample. For the same reason the thermoelectric power was measured down to 240 K.

3. Results

The variation of electrical resistivity as a function of pressure is shown in figure 3. The room temperature and atmospheric value of resistivity ρ_0 is 2.77×10^4 ohm-cm, which

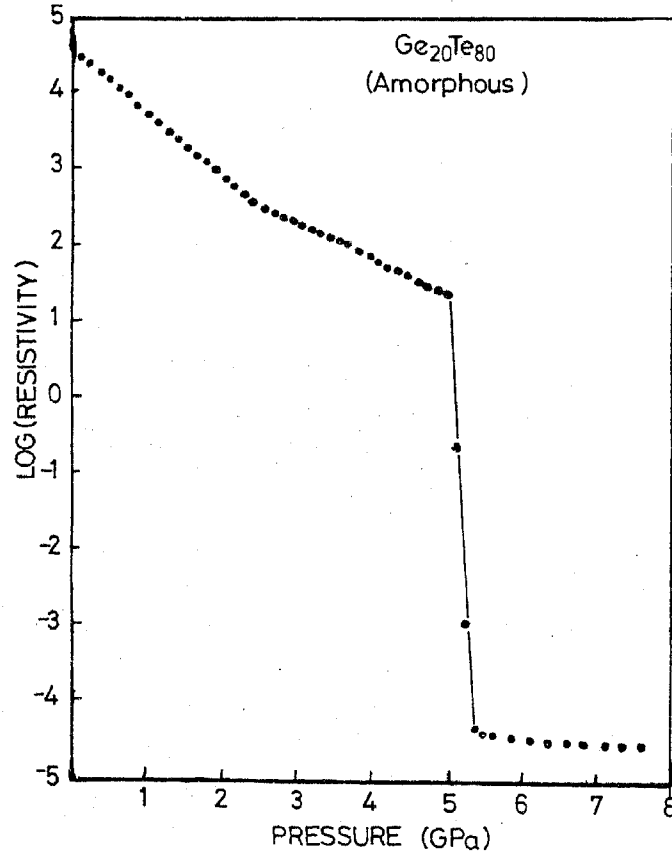


Figure 3. Variation of electrical resistivity as a function of pressure for amorphous Ge₂₀Te₈₀ sample.

is in fairly good agreement with the reported value (Nakamura *et al* 1975). The change in the dimensions of the sample under high pressure was not considered in calculating the resistivity at high pressures. The effect of this on the resistivity is small. The resistivity decreases exponentially with the increase of pressure by three orders of magnitude up to 5 GPa, and at nearly 5 GPa the resistivity drops suddenly by six orders of magnitude. Beyond 5.5 GPa the variation of resistivity with the increase of pressure is very small.

Figure 4 shows the variation of electrical resistivity as a function of pressure for polycrystalline $\text{Ge}_{20}\text{Te}_{80}$ sample. The room temperature and atmospheric pressure value of resistivity is roughly 5×10^{-3} ohm-cm. The resistivity of crystalline $\text{Ge}_{20}\text{Te}_{80}$ also decreases with increase of pressure, but the pressure coefficient of electrical resistivity is much less when compared to that in glass. At 7 GPa, the resistivity jumps by one order of magnitude, and remains constant for further increase of pressure. The value of the resistivity after the transition (in both cases) is very much less than the Mott's maximum metallic resistivity (Mott 1970).

The variations of electrical resistivity as a function of temperature at different clamped pressures are shown in figures 5, 6 and 7. For pressures up to 5 GPa, the variation of resistivity obeys the relation

$$\rho(T) = \rho_0 \exp(\Delta E/kT), \quad (1)$$

where ρ_0 = the pre-exponential factor, ΔE = the activation energy for electronic conduction, k = Boltzmann's constant and T = the absolute temperature. The ΔE and ρ_0 values for different pressures are tabulated in table 1.

Figure 8 shows the variation of activation energy ΔE as a function of pressure. The pressure coefficient of activation energy is -0.082 eV/GPa. Figure 9 shows the variation of thermoelectric power as a function of temperature. The thermoelectric power obeys the relation

$$S = \frac{k}{e} \left(\frac{E_c - E_F}{kT} + A \right), \quad (2)$$

where k = Boltzmann's constant, $A = 1$ and T = the temperature. From the plot of S vs $(1000/T)$, we find the slope and hence the activation energy for the electronic conduction as 0.40 eV.

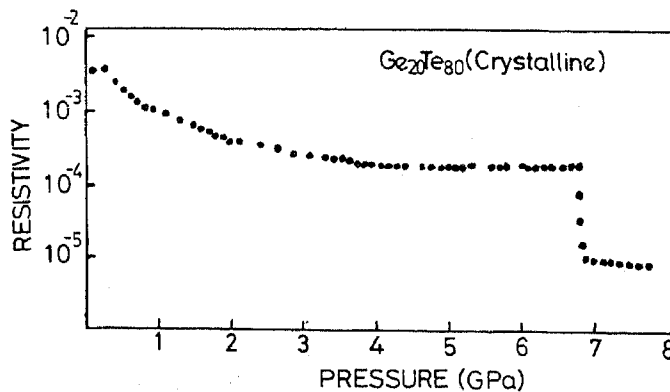


Figure 4. Variation of electrical resistivity of crystalline $\text{Ge}_{20}\text{Te}_{80}$ sample as a function of pressure.

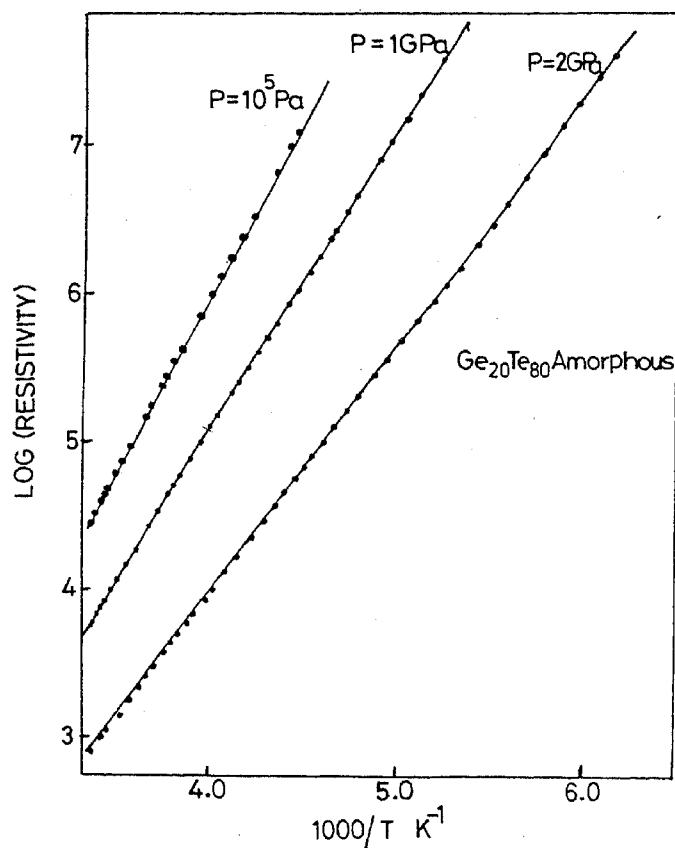


Figure 5. Semilog plot of electrical resistivity vs $(10^3/T)$ for $\text{Ge}_{20}\text{Te}_{80}$ glass at pressures 10^5 Pa, 1 and 2 GPa.

Figure 10 shows the x-ray diffraction pattern of the pressure quenched sample at a pressure of 7 GPa. The peaks clearly indicate that the high pressure phase of $\text{Ge}_{20}\text{Te}_{80}$ glass is a face-centred cubic structure with a lattice constant 6.42 Å. In crystalline $\text{Ge}_{20}\text{Te}_{80}$ sample, similar pressure-quenching experiments could not be performed as the transition is reversible in the crystalline sample. In these cases, *in situ* high pressure x-ray studies are required.

4. Discussion

The primary effect of pressure is to decrease the interatomic distances and hence the compression gives rise to changes in electronic structure and sometimes to a semiconductor-to-metal transition. Because the amorphous or glassy form is thermodynamically unstable, most of the glassy materials will undergo transition from amorphous to crystalline form with the increase of pressure. The value of the transition pressure depends upon the nature of the bond. For example, chalcogenide glasses become metallic under high pressure with a continuous decrease in optical gap and resistivity even as they retain their molecular structure (Minomura 1982; Sakai and Fritzsche 1977; Bhatia *et al* 1984; Parthasarathy *et al* 1984c). Some chalcogenide glasses do show a completely different behaviour, where the resistivity continuously decreases

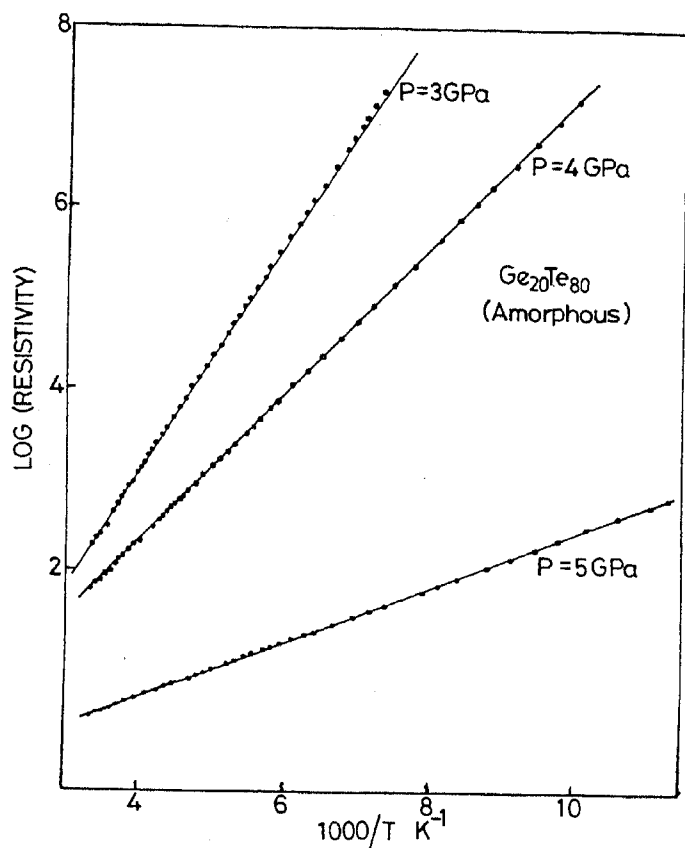


Figure 6. Semilog plot of electrical resistivity vs $(10^3/T)$ for $\text{Ge}_{20}\text{Te}_{80}$ glass for pressures 3, 4 and 5 GPa.

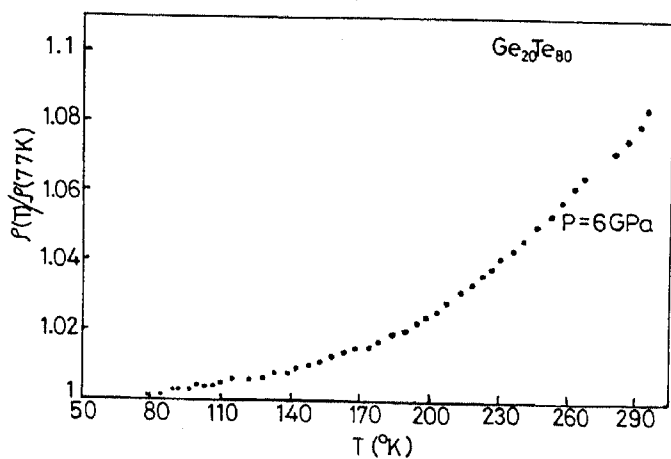


Figure 7. Variation of normalised resistivity $(\rho(T)/\rho(300\text{K}))$ as a function of temperature for $\text{Ge}_{20}\text{Te}_{80}$ sample at 6 GPa pressure.

Table 1. Values of the activation energies E and the pre-exponential factors obtained from the Arrhenius formula $\rho = \rho_0 \exp(\Delta E/kT)$ at different clamped pressures.

Pressure (GPa)	ΔE (eV)	ρ_0 (ohm cm)
10^{-4}	0.47	3.52×10^{-4}
1	0.40	1.07×10^{-3}
2	0.33	2.27×10^{-3}
3	0.25	1.205×10^{-2}
4	0.16	0.1294
5	0.06	0.2464

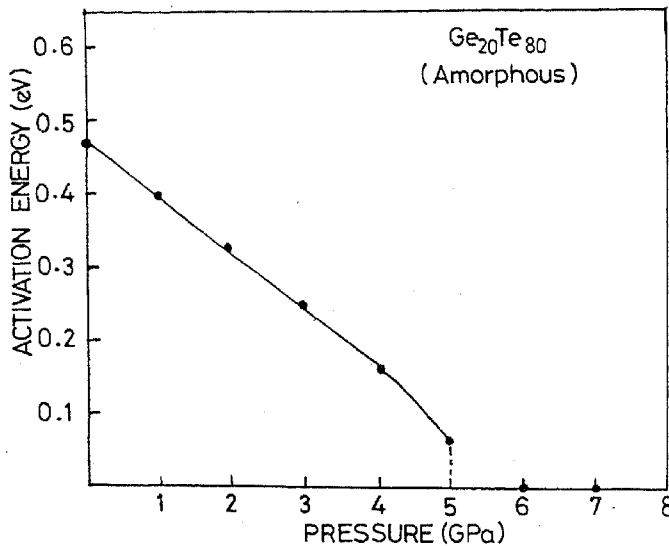


Figure 8. Variation of activation energy as a function of pressure for $\text{Ge}_{20}\text{Te}_{80}$ glass.

with the increase of pressure and at a particular pressure, the resistivity drops by several orders of magnitude (Fuhs *et al* 1973; Parthasarathy *et al* 1984c; Prasad *et al* 1984). In tetrahedrally bonded glasses the pressure-induced transitions are discontinuous, accompanied by changes in structure to a higher coordination.

The pressure coefficient of the optical gap in chalcogenide glasses lies in between -0.1 and -0.2 eV/GPa. The activation energy ΔE , derived from the temperature dependence of resistivity, and the optical gap E_0 are related by $\Delta E \approx 1/2 E_0$ indicating that the Fermi level lies near the centre of the gap (Sakai and Fritzsche 1977). The pressure coefficient value of the electrical activation energy should therefore lie between -0.05 and -0.1 eV/GPa. From figure 8, we get the value of pressure coefficient of activation energy as -0.082 eV/GPa which lies in the acceptable range. This indicates that the decreases in the electrical resistivity (figure 4) under pressure arises from a gradual decrease in the gap; but the pressure dependence of the resistivity is more complicated because the resistivity depends not only upon the gap but also on the mobility and the position of the Fermi level (Paul and Warschauer 1963). Therefore an

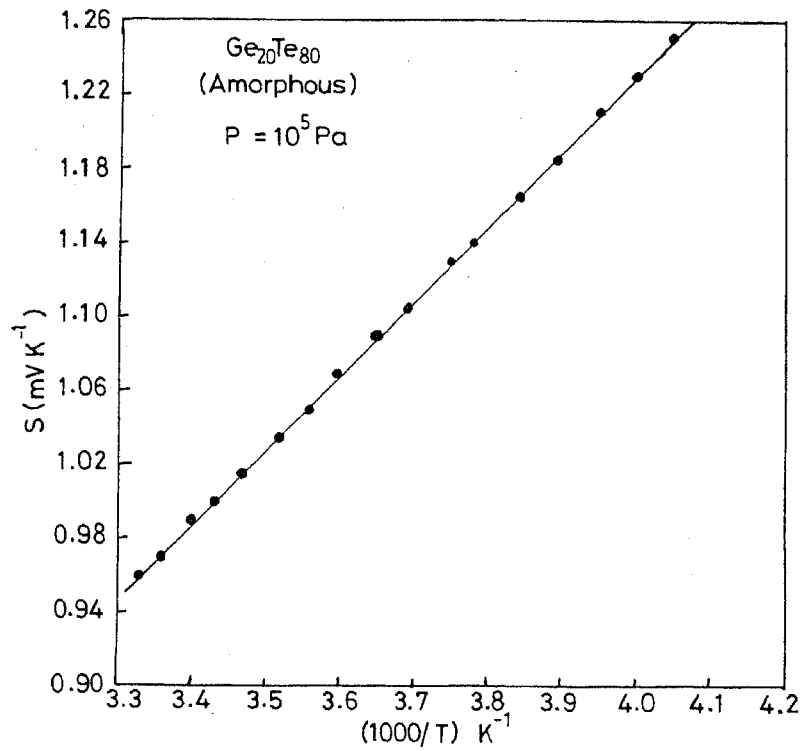


Figure 9. Plot of thermoelectric power S vs $(10^3/T)$ for Ge₂₀Te₈₀ glass at atmospheric pressures.

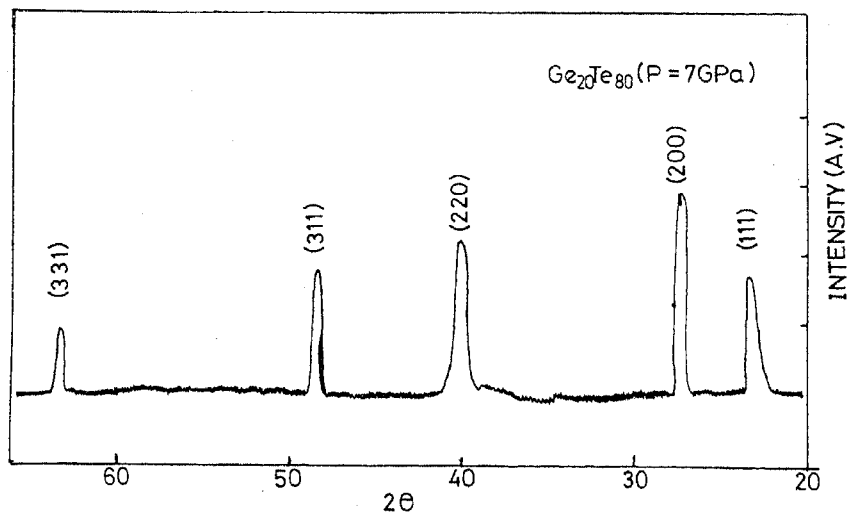


Figure 10. x-ray diffractogram of pressure quenched Ge₂₀Te₈₀ sample.

independent experiment on the pressure dependence of mobility is required to get a clear understanding about the behaviour of the resistivity under high pressure.

The electronic conduction in the sample (figures 6 and 7) at low pressures (up to 5 GPa) is of a thermally-activated type. By fitting the data of temperature dependence of electrical resistivity into (1), we get the values of pre-exponential factor ρ_0 and the activation energy ΔE . These values are tabulated in table 1. Mott (1970) has made an estimate of ρ_0 for the extended state conduction, where the transport is by carriers excited beyond the mobility edges into nonlocalized (extended) states at E_c or E_v . In general ρ_0 lies between 0.1 and 10^{-4} ohm-cm in most amorphous semiconductors (Nagels 1979). From table 1, we see that at all pressures the conduction occurs through the extended states and hence a decrease in the activation energy represents the decrease of fundamental band gap with the increase of pressure. The increase of ρ_0 with increase of pressure may be attributed to the increase of the width of the localized states with increase of pressure.

The resistivity of the sample after the transition roughly 3×10^{-5} ohm-cm, which is much lower than the value of Mott's (1970) maximum metallic resistivity. Figure 7 shows the positive temperature coefficient of resistivity at 6 GPa pressure. The positive temperature coefficient of resistivity and the numerical value of the resistivity confirms the metallic state of the sample at high pressure.

In crystalline $\text{Ge}_{20}\text{Te}_{80}$ sample the semiconductor-to-metal transition is observed at 7 GPa pressure (figure 5). The crystalline $\text{Ge}_{20}\text{Te}_{80}$ contains the two phases GeTe, with a distorted NaCl structure, and Te with a trigonal structure (see figure 2). We know that crystalline Te undergoes a semiconductor-to-metal transition at 4 GPa pressure (Bridgman 1952) and crystalline Ge undergoes a semiconductor-to-metal transition at 10 GPa pressure. So we should expect the transition for crystalline $\text{Ge}_{20}\text{Te}_{80}$ between 4 GPa and 10 GPa. Our experimental observation is in good agreement with the expected value. It has been suggested that the covalent-metallic transitions in tetrahedrally bonded crystalline and amorphous semiconductors under pressure are connected with the shear instabilities (Minomura 1982) and the deviations of bond angles and dihedral angles in the amorphous semiconductors cause the lower transition pressure. The temperature coefficient of resistivity of crystalline $\text{Ge}_{20}\text{Te}_{80}$ is positive at all the pressures including the atmospheric pressure, because GeTe is a degenerate semiconductor which is superconducting at very low temperatures (Builova and Sandomirskii 1969).

Important information about the transport mechanism in amorphous semiconductors can sometimes be obtained from thermoelectric power data. At room temperature the thermopower of our amorphous $\text{Ge}_{20}\text{Te}_{80}$ sample is $960 \mu\text{V}/\text{K}$ which shows that the conduction process is dominated by holes. The temperature dependence of thermopower follows the relation (2) (figure 9) which implies the conduction in the extended states (Nagels 1979). The activation energy from the slope of the S vs $(10^3/T)$ plot was found to be 0.40 eV. From table 1 we know that the activation energy derived from $\ln \rho$ vs $(10^3/T)$ plot is equal to 0.47 eV. In principle we should get the same value of activation energies in both cases. However a difference in slopes, of the order of 0.1 to 0.15 eV, was observed between the conductivity and the thermopower curves in other chalcogenide glasses also. In our experiment the value of difference was found to be 0.07 eV, which is well within the range earlier observed in other glasses.

The discontinuous transition in glassy $\text{Ge}_{20}\text{Te}_{80}$ sample leads us to the study of x-ray diffraction and electron microscopy of the pressure quenched sample. The x-ray

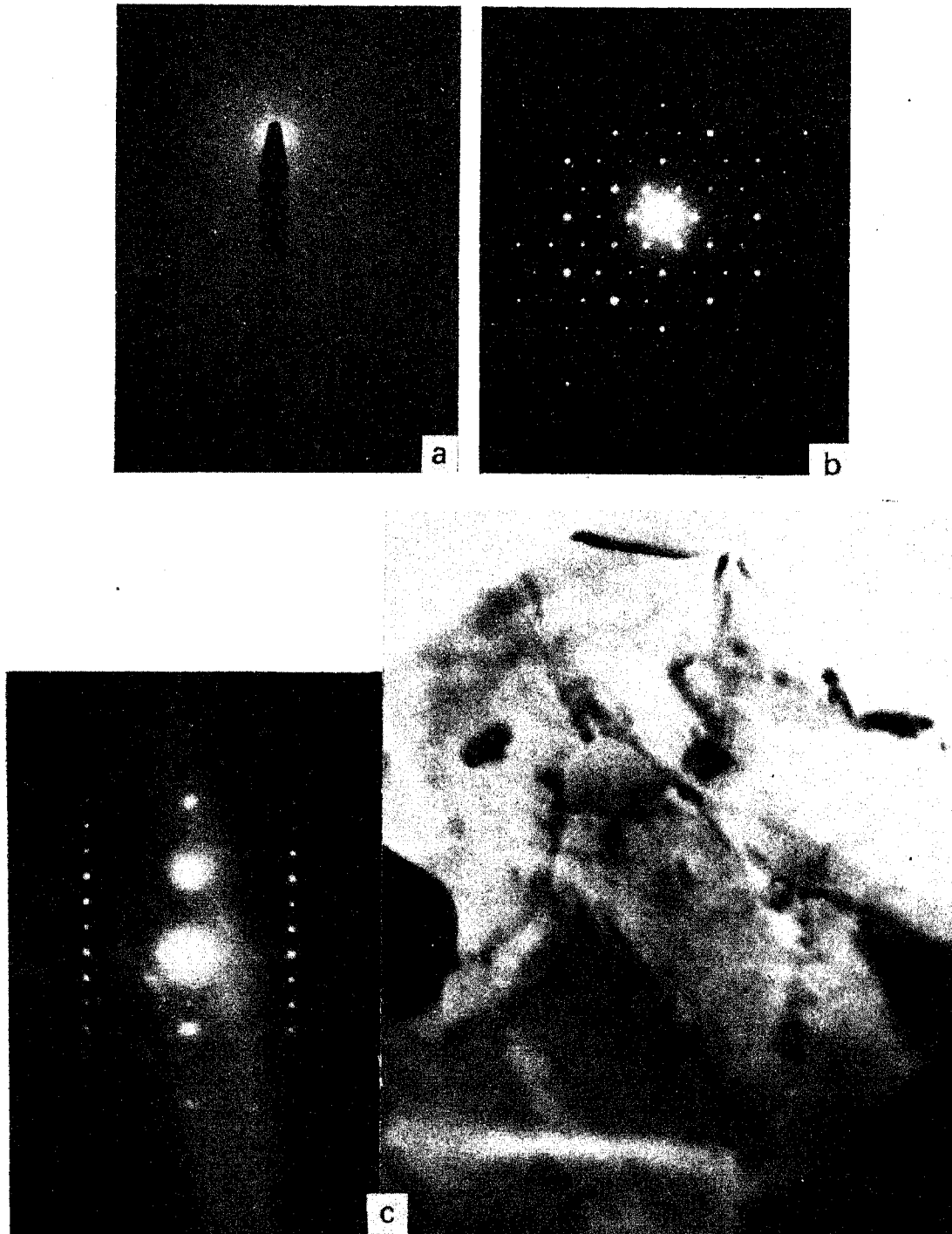


Figure 11. Electron diffraction pattern of (a) amorphous $\text{Ge}_{20}\text{Te}_{80}$ sample, (b) temperature induced crystalline phase of $\text{Ge}_{20}\text{Te}_{80}$ and (c) pressure induced crystalline phase of $\text{Ge}_{20}\text{Te}_{80}$ sample, (d) TEM micrograph of the pressure quenched $\text{Ge}_{20}\text{Te}_{80}$ sample.

diffraction pattern (figure 10) shows that the pressure-quenched sample has a face-centred cubic structure with $a = 6.42$ Å. It is really surprising that the pressure-induced crystallization is a single cubic phase, which is more stable than the two phases obtained in the temperature induced crystallization. Figure 11 shows the electron diffraction pattern of amorphous, the room pressure crystalline phase, and the pressure-quenched crystalline phase. It is seen that the room temperature crystalline phase consists of two phases *viz.*, Te (trigonal) and GeTe (distorted NaCl structure). On the other hand the pressure-quenched crystalline phase is recognised as face-centred cubic with $a = 6.42$ Å (figure 11c). The micrograph of the pressure quenched phase is also shown in figure 11(d). This micrograph indicates the presence of pressure-induced defects in the high pressure crystalline phase of $\text{Ge}_{20}\text{Te}_{80}$ alloy. Both x-ray diffraction and electron diffraction techniques confirm the cubic phase of the pressure-quenched $\text{Ge}_{20}\text{Te}_{80}$ sample. They also assist in establishing the amorphous nature of the initial starting glassy samples.

5. Conclusions

In this paper we have reported the semiconductor-to-metal transitions in amorphous and crystalline $\text{Ge}_{20}\text{Te}_{80}$ sample. In the amorphous sample the transition is accompanied by a structural transformation from the amorphous to a face-centered cubic structure.

Acknowledgements

The authors are thankful to DST and CSIR, Government of India, for their financial support and the referees for useful comments.

References

- Bandyopadhyay A K, Nalini A V, Gopal E S R and Subramanyam S V 1980 *Rev. Sci. Instrum.* **51** 136
 Bhatia K L, Parthasarathy G and Gopal E S R 1983 *J. Non-Cryst. Solids*. **59 & 60** 1019
 Bridgman P W 1952 *Proc. Am. Acad. Arts. Sci.* **81** 169
 Builova N M and Sandomirskii V B 1969 *Sov. Phys. Usp.* **97** 119
 Cornet J 1976 *Proc. sixth. int. conf. on amorphous and liquid semiconductors*. 18–24 Nov. 1975, Leningrad (ed) B T Kolomiets p 72
 Elliot S R, Davis E A and Pitt G D 1977 *Solid State Commun.* **22** 481
 Fuhs W, Schlotter P and Stuke J 1973 *Phys. Status Solidi* **57** 587
 Geetha Ramani, Giridhar A, Singh A K and Rao K J 1979 *Philos. Mag.* **B29** 385
 Jhonson R T Jr and Quinn R K 1978 *J. Non-Cryst. Solids* **28** 273
 Minomura S 1982 in *Amorphous semiconductors technologies and devices*. (ed.) Y Hamakawa (Amsterdam: North-Holland)
 Mott N F 1970 *Philos. Mag.* **22** 7
 Nagels P 1979 in *Amorphous semiconductors* (ed.) M H Brodsky (New York: Springer-Verlag) p 113
 Nakamura Y, Numata M, Hoshino H and Shimoji M 1975 *J. Non-Cryst. Solids* **17** 259
 Parthasarathy G and Gopal E S R 1984 *Bull. Mater. Sci.* (in press)
 Parthasarathy G, Bandyopadhyay A K, Gopal E S R and Subbanna G N 1984a *J. Mater. Sci. Lett.* **3** 97
 Parthasarathy G, Bandyopadhyay A K and Gopal E S R 1984b *Proc. Indo-Soviet Conference on Low Temp. Physics*. 11–15 Jan. 1984 Bangalore (to be published)

- Parthasarathy G, Gopal E S R, Lakshmikummar S T 1984c *J. Noncryst. Solids* (to be published)
Paul W and Warschauer D M 1963 *Solids under pressure* (New York: McGraw Hill) p. 179.
Prasad M V N, Parthasarathy G, Asokan S and Gopal E S R 1984 *Pramana* **23** 31
Sakai N and Fritzsche H 1977 *Phys. Rev.* **B15** 973
Shimomura O, Minomura S, Sakai N, Asaumi K, Tamura K, Fukushina J and Endo H 1974 *Philos. Mag.* **29**
547